

Tracklet-Switch Adversarial Attack against Pedestrian Multi-Object Tracking Trackers

Delv Lin*, Qi Chen*, Chengyu Zhou, and Kun He†

Abstract—Multi-Object Tracking (MOT) has achieved aggressive progress and derived many excellent deep learning trackers. Meanwhile, most deep learning models are known to be vulnerable to adversarial examples that are crafted with small perturbations but could mislead the model prediction. In this work, we observe that the robustness on the MOT trackers is rarely studied, and it is challenging to attack the MOT system since its mature association algorithms are designed to be robust against errors during the tracking. To this end, we analyze the vulnerability of popular MOT trackers and propose a novel adversarial attack method called Tracklet-Switch (TraSw) against the complete tracking pipeline of MOT. The proposed TraSw can fool the advanced deep pedestrian trackers (*i.e.*, FairMOT and ByteTrack), causing them fail to track the targets in the subsequent frames by perturbing very few frames. Experiments on the MOT-Challenge datasets (*i.e.*, 2DMOT15, MOT17, and MOT20) show that TraSw can achieve an extraordinarily high success attack rate of over 95% by attacking only four frames on average. To our knowledge, this is the first work on the adversarial attack against the pedestrian MOT trackers. Code is available at <https://github.com/JHL-HUST/TraSw>.

Index Terms—Vulnerability-oriented attack, adversarial attack, multi-object tracking, pedestrian MOT tracker, tracklet switch

I. INTRODUCTION

OWING to the rapid development of Deep Neural Networks (DNNs), Visual Object Tracking (VOT) [1], [2] has been dramatically boosted in recent years with a wide range of applications, such as autonomous driving [3], intelligent monitoring [4], human-computer interaction [5], *etc.* Researches on VOT fall into two categories, namely Single-Object Tracking (SOT) and Multi-Object Tracking (MOT). The goal of SOT is to track a single target given in the first frame of the video, while MOT aims to track all the targets of interest in an unsupervised setting and link the objects in different frames to form their trajectories.

On the other hand, deep learning models of various computer vision tasks are known to be vulnerable to adversarial examples [6]–[10], which are crafted with imperceptible perturbations but lead the models to wrong predictions. Studying the generation of adversarial examples can help promote the understanding of internal mechanism on DNNs, dig out their potential risks, and assist us to design robust deep learning systems. Therefore, adversarial attacks have been extensively studied in many computer vision tasks, such as

image classification [8], [9], [11]–[14], object detection [15]–[18], semantic segmentation [19]–[21], *etc.* Current adversarial attack methods of VOT are mainly concentrated in Single-Object Tracking [22]–[24], and there is little work on attacking the Multi-Object Tracking system. To our knowledge, there exists only one work that does MOT adversarial attack on autonomous driving [25].

In this work, we focus the adversarial attacks on pedestrian tracking and investigate the robustness of these MOT trackers. The underlying reasons for this specification are twofold. First, the previous adversarial study, *tracker hijacking*, is focused on vehicle tracking [25], in which the attacked models are the detection-based trackers. But motion-and-appearance-based trackers [26]–[28] are also popular and the performance of the detection-based trackers has been improved significantly over the years. In Table I, we observe that for the recent state-of-the-art detection-based tracker, ByteTrack [29], the attack success rate of *tracker hijacking* is much lower than that of the method proposed in this paper, especially under the crowded tracking scenarios. Second, most of the current MOT researches focus on pedestrian tracking. According to the statistics in [30], at least 70% of the current MOT research efforts are devoted to pedestrians, but there is no corresponding adversarial study.

A typical MOT tracker addresses the tracking in two steps [30]–[32]. First, the tracker locates all the objects in each frame. Then, according to the metric of similarity, each detected object is associated with a trajectory. It is important and challenging to consistently label the objects over time, especially in complex scenes with occlusion and interaction of objects. Great efforts have been devoted to improve the tracking robustness [26], [31], [33]–[35].

Attacking these trackers poses new challenges due to their memory characteristics. Specifically, the continuous tracking process allows the tracker to save the moving states of the trajectories for a long period (*e.g.*, 30 frames). As a result, if an object disappears for a few frames, it actually has little impact on the final trajectory. Moreover, the corresponding trajectory will be removed only if the tracking object disappears for sufficient frames (*e.g.*, 30 frames). Simply removing or tampering with the objects is quite inefficient. In Fig. 4, we find that even if the attacked frames are up to 20, the attack success rate of the object detection attacks that hide objects is hard to reach 90%.

To address the above challenges, we propose a novel attack method called the *Tracklet-Switch* (TraSw). In a nutshell, our method learns an effective perturbation generator to make the tracker confuse intersecting trajectories by attacking as few

The authors are with Huazhong University of Science and Technology, Hubei, China. E-mail: {derrylin, bloom24, hust_zcy, brooklet60}@hust.edu.cn.

The first two authors contribute equally.

Corresponding author: Kun He.

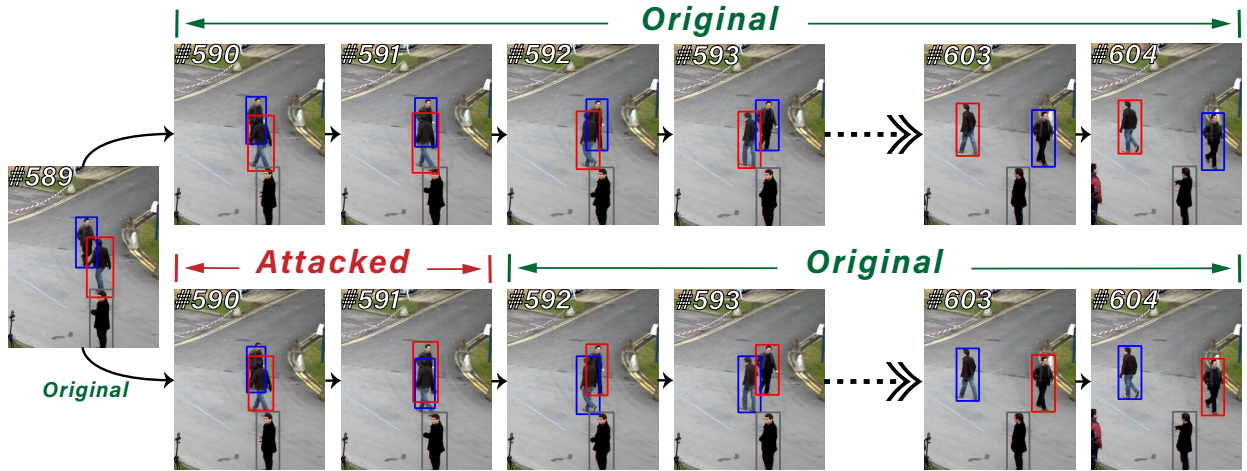


Fig. 1: The illustration of the adversarial effect to tracking. *First row*: the original video clips. *Second row*: the adversarial video clips. The blue boxes represent the detected objects of the 19th trajectory, the red boxes represent those of the 24th trajectory, and the gray boxes represent the 16th trajectory not participated in the attack. Attacking two frames in the example video, TraSw switches the trajectories of the 19th and the 24th. After the attack, the exchanged state can hold until the end of the video.

as one frame, as illustrated in Fig. 1, and the error state can transfer across frames until the end of the sequences. In our method, we propose two novel losses, *PushPull* and *CenterLeaping*. *PushPull* works on the re-identification (re-ID) branch, while *CenterLeaping* works on the detection branch. They can work together or separately to accommodate different kinds of MOT trackers (e.g., detection-based trackers, motion-and-appearance-based trackers).

To better illustrate the effectiveness and efficiency of TraSw, we choose three MOT-Challenge datasets, i.e., 2DMOT15, MOT17 and MOT20 [36]–[38], for evaluation, and compare TraSw with representative object detection adversarial attack methods [15], [22], [23], [39], as well as the MOT adversarial attack method, *tracker hijacking* [25]. Experiments show that our method achieves a significantly higher success rate with fewer attacked frames and smaller perturbations.

II. RELATED WORK

A. Multi-Object Tracking

Multi-Object Tracking aims to locate and identify the targets of interest in the video and estimate their movements in the subsequent frames [30], [31], [33], [35], [40]–[43], such as pedestrians on the street, vehicles on the road, or animals on the ground. The mainstream MOT trackers break the tracking into two steps: 1) the detection stage, where objects are located in the images, 2) the association stage, where the objects are linked to the trajectories.

The MOT trackers are expected to keep consistent track of each object over time; that is, each object should be assigned a unique track ID which stays constant throughout the whole sequence. To ensure as accurate tracking as possible, the tracker uses tracklets to maintain the moving states of the existing trajectories (e.g., position, velocity, and appearance). For a coming frame, the tracker compares the detected objects with tracklets to determine whether it belongs to an existing trajectory or is a new trajectory. The matching process between the tracklets and the detected objects is regarded as a bipartite

matching problem based on the pair-wise similarity affinity matrix between all the tracklets and detected objects [25]. Most trackers use the motion information for evaluation. The commonly used motion similarity evaluation metric is Intersection-over-Union (IoU), which measures the spatial overlapping between two bounding boxes (bboxes). Some trackers also calculate the appearance affinity matrix to measure their appearance similarity. For those trackers, that only utilize motion flows to track objects, we call them detection-based trackers [29], [33], [44]. And for those using both motion and deep appearance feature of the object for matching, we call them motion-and-appearance-based trackers [26], [31], [34].

After that, the matched tracklets will be updated (e.g., motion state, appearance state), and the unmatched objects will be initialized as new trajectories. The unmatched tracklets won't be removed immediately, instead they are moved to the lost pool. If objects of the lost tracklets reappear, the corresponding tracklets will be updated and put back into the tracking pool. Otherwise, if the missing tracklet reaches the maximum cache period (e.g., 30 frames), the unmatched tracklet will be completely removed. Even if the target reappears later, it will be regarded as an entirely new trajectory.

B. Adversarial Attacks on Visual Object Tracking

Adversarial Attacks on Single-Object Tracking. The SOT tracker is informed of the tracking target in the first frame, and the goal is to predict the position and size of the tracking target in subsequent frames [45]–[47].

Since the tracking template is given in the first frame, if the tracking template is wrong, the tracker cannot track the target. The early SOT attack method, one-shot attack [22], aims to disturb the template by adding perturbations on the template patch in the initial frame. To get the perturbation, the attacker needs to iterate over every frame in the video to compute the perturbation. However, traversing all the frames is inefficient and unpractical.

Subsequently, Yan *et al.* [23] propose a *cooling-shrinking* attack method to fool the SiamPRN-based trackers [45], [46] by training a perturbation generator to craft noise to interfere the search regions so as to make the target invisible to the trackers. More recently, Jia *et al.* [24] present a decision-based black-box attack method, called IoU attack, that aims to gradually decrease the IoU score between the bbox of the clean image and the bbox of the adversarial sample, which leads the prediction deviating from its original trajectory. These methods need to attack all the video frames. As the attacked target is determined in SOT, the number of attacks is relatively small, and valid attack samples can be obtained quickly. However, in MOT, the tracking quantity and tracking template vary along the frames. It is difficult to obtain effective adversarial examples by simply transplanting the SOT attack methods.

Adversarial Attacks on Multi-Object Tracking. Compared with SOT, there is little work on attacking MOT. There is only one MOT attack method proposed on autonomous driving, called *tracker hijacking* [25]. By fabricating the bboxes toward the expected attacker-specified direction and erasing the original bboxes, the attacked object deviates from its original trajectory. As a result, the successful adversaries can move an object out of (into) the view of an autonomous vehicle. *Tracker hijacking* attacks those detection-based trackers [25], [30], that crafts adversarial examples to fool the object detection module.

For reference, we provide a comparison of *tracker hijacking* and our proposed TraSw on the state-of-the-art pedestrian trackers.

III. PRELIMINARIES

In this work, we choose FairMOT [35] and ByteTrack [29] as our main target models for attack. As FairMOT and ByteTrack share similar structures except for the re-ID branch in FairMOT, we primarily focus on introducing FairMOT to illustrate our proposed method. In this section, we first introduce the overview of FairMOT, then we provide the problem definition of adversarial attack on MOT pedestrian trackers.

A. Overview of FairMOT

FairMOT stands out among many trackers by achieving a good trade-off between accuracy and efficiency. As shown in Fig. 2, FairMOT consists of two homogeneous branches for object detection and feature extraction, and follows the standard online association algorithm.

Detection Branch. The anchor-free detection branch of FairMOT is built on CenterNet [48], consisting of the heatmap head, box-size head and center-offset head. Denote the ground-truth (GT) bbox of the i -th object in the t -th frame as $box_t^i = (x_1^{t,i}, y_1^{t,i}, x_2^{t,i}, y_2^{t,i})$. The i -th object's center $(c_x^{t,i}, c_y^{t,i})$ is computed by $c_x^{t,i} = \frac{x_1^{t,i} + x_2^{t,i}}{2}$ and $c_y^{t,i} = \frac{y_1^{t,i} + y_2^{t,i}}{2}$. The response location of the center on the heatmap can be obtained by dividing the stride (which is 4 in FairMOT) ($\lfloor \frac{c_x^{t,i}}{4} \rfloor, \lfloor \frac{c_y^{t,i}}{4} \rfloor$). The heatmap value indicates the probability of presence of an object centering at this point. The GT box size and center offset are computed by $(x_2^{t,i} - x_1^{t,i}, y_2^{t,i} - y_1^{t,i})$ and $(\frac{c_x^{t,i}}{4} - \lfloor \frac{c_x^{t,i}}{4} \rfloor, \frac{c_y^{t,i}}{4} - \lfloor \frac{c_y^{t,i}}{4} \rfloor)$, respectively.

Re-ID Branch. The re-ID branch generates the re-ID features of the objects. Denote the feature map as $feat_t \in \mathbb{R}^{512 \times H \times W}$. The re-ID feature $feat_t^i \in \mathbb{R}^{512}$ represents the feature vector of the i -th object, whose L_2 norm equals 1.

Association. FairMOT follows the association strategy in [31]. The tracker uses tracklet to describe the trajectory's appearance state a_t^i and motion state $m_t^i = (x^{t,i}, y^{t,i}, \gamma^{t,i}, h^{t,i}, \dot{x}^{t,i}, \dot{y}^{t,i}, \dot{\gamma}^{t,i}, \dot{h}^{t,i})$ in the t -th frame, where $(x^{t,i}, y^{t,i})$ indicates the predicted center, $h^{t,i}$ the height and $\gamma^{t,i}$ the aspect ratio, followed by their velocity information. The initial appearance state a_0^i is initialized with the first observation's appearance embedding $feat_0^i$ of object i , and a_t^i is updated by:

$$a_t^i = \alpha \cdot a_{t-1}^i + (1 - \alpha) \cdot feat_t^i, \quad (1)$$

where $feat_t^i$ is the appearance embedding of the matched object in the t -th frame. The bbox information in the motion state m_t^i is updated by the predicted center $(x^{t,i}, y^{t,i})$, height $h^{t,i}$ and aspect ratio $\gamma^{t,i}$ in the t -th frame, and velocity information $(\dot{x}^{t,i}, \dot{y}^{t,i}, \dot{\gamma}^{t,i}, \dot{h}^{t,i})$ is updated by the Kalman filter.

For a coming frame, we compute the pair-wise similarity matrix between the observed objects in the t -th frame and the tracklets maintained by the tracklet pool TrP_{t-1} . Then the association problem is solved by the Hungarian algorithm using the final cost matrix:

$$d_t = \lambda \cdot d_{box}(K(m_{t-1}), box_t) + (1 - \lambda) \cdot d_{feat}(a_{t-1}, feat_t), \quad (2)$$

where box_t and $feat_t$ denote the detected bboxes and features in the t -th frame. $K(\cdot)$ represents the Kalman filter that uses motion state m_{t-1} to predict the expected positions of the trajectories in the t -th frame, and $d_{box}(\cdot)$ stands for a certain measurement of the spatial distance, which is the Mahalanobis distance in FairMOT, and $d_{feat}(\cdot)$ represents the cosine similarity.

B. Problem Definition

Let $V = \{I_1, \dots, I_t, \dots, I_N\}$ denote the sequence frames of a video. Consider a scenario where the tracker detects two trajectories intersected at frame t . Denote the two trajectories as $T_i = \{O_{s_i}^i, \dots, O_t^i, \dots, O_{e_i}^i\}$ and $T_j = \{O_{s_j}^j, \dots, O_t^j, \dots, O_{e_j}^j\}$. Their bboxes and features are $B_k = \{box_{s_k}^k, \dots, box_t^k, \dots, box_{e_k}^k\}$ and $F_k = \{feat_{s_k}^k, \dots, feat_t^k, \dots, feat_{e_k}^k\}$ where $k \in \{i, j\}$, $box_t^k \in \mathbb{R}^4$ and $feat_t^k \in \mathbb{R}^{512}$.

Then we define the adversarial video as $\hat{V} = \{I_1, \dots, I_{t-1}, \hat{I}_t, \dots, \hat{I}_{t+n-1}, I_{t+n}, \dots, I_N\}$, where I, \hat{I} indicate the original frame and adversarial frame, respectively. For the attack trajectory T_i , we call T_j , that overlaps with T_i in the t -th frame, the screener trajectory. The adversarial video \hat{V} misleads the tracker to estimate trajectory i as $\hat{T}_i = \{O_{s_i}^i, \dots, O_{t-1}^i, O_t^j, \dots, O_{t+n-1}^j, O_{t+n}^i, \dots, O_{e_j}^j\}$. The goal is to attack the frame sequences to make the tracking of trajectory T_i change to that of T_j since the t -th frame.

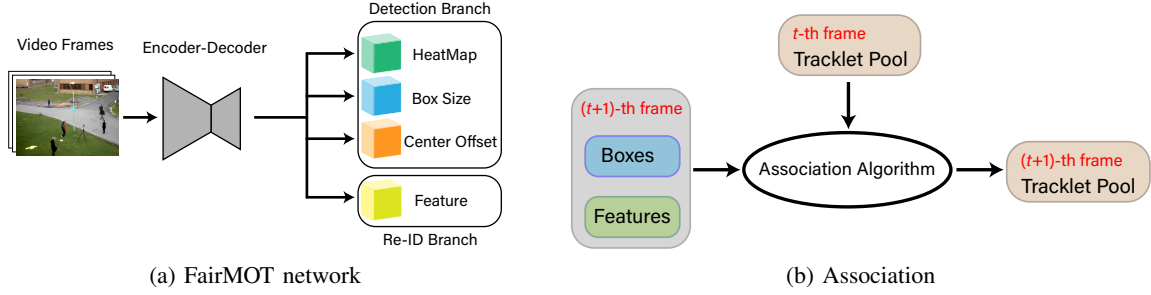


Fig. 2: Overview of FairMOT, a typical MOT tracker as our main target model.

IV. THE TRASW ADVERSARIAL ATTACK

In this section, we propose a novel method called the *Tracklet-Switch* (TraSw) adversarial attack against the pedestrian trackers, which aims to switch the tracklets of two intersecting trajectories in the video frames. In Sec. IV-A and Sec. IV-B, we propose the *PullPush* loss and the *CenterLeaping* technique. Then, we present the overall pipeline of TraSw in Sec. IV-C.

A. Feature Attack with Push-Pull Loss

The tracker distinguishes the objects through a combination of motion and appearance similarity. When objects are close to each other, the tracker relies more on the re-ID features to distinguish the objects. Therefore, we can reform the re-ID features of the objects to make them similar to another tracklet. Inspired by the triplet loss [49], we design the *PushPull* loss to push away the attack (screener) feature and pull the screener (attack) feature, as follows:

$$\mathcal{L}_{pullpush}(a_{t-1}^i, a_{t-1}^j, feat_t^i, feat_t^j) = \sum_{k \in \{i,j\}} d_{feat}(a_{t-1}^k, feat_t^{\tilde{k}}) - d_{feat}(a_{t-1}^k, feat_t^k), \quad (3)$$

where $d_{feat}(\cdot)$ denotes the cosine similarity, a_{t-1}^i and a_{t-1}^j represent the appearance feature of the attack and screener tracklets, $feat_t^i$ and $feat_t^j$ represent the feature of the attack and screener objects, and k represents the attack (screener) ID while \tilde{k} represents the screener (attack) ID, whose object overlaps most with object k (i.e., $\tilde{i} = j$ and $\tilde{j} = i$). The loss will make $feat_t^k$ dissimilar to tracklet k and make $feat_t^{\tilde{k}}$ similar to tracklet k (see Fig. 3a).

Specifically, in FairMOT, the object's feature is extracted from the feature map $feat_t \in \mathbb{R}^{512 \times H \times W}$ according to the predicted object center (x, y) . Considering the surrounding locations of the center that may be activated, we calculate the appearance cost within a nine-block box location (as illustrated in Fig. 3b) for a more stable attack. So the final *PushPull* loss for FairMOT is as follows:

$$\mathcal{L}_{pp} = \sum_{(dx, dy) \in \mathcal{B}} \mathcal{L}_{pullpush}(a_{t-1}^i, a_{t-1}^j, feat_t^{i,(dx,dy)}, feat_t^{j,(dx,dy)}), \quad (4)$$

where \mathcal{B} indicates a set of offsets in the nine-block box location, $feat_t^{i,(dx,dy)}$ and $feat_t^{j,(dx,dy)}$ represent the feature extracted around the center of the attack and screener object, respectively.

B. Detection Attack with Center Leaping

Attacking the features of intersection trajectories can generally fool the tracker. But it may be insufficient when the spatial distance is too large to switch, and some trackers only use the detection result for the association.

In order to adjust the distance between objects and tracklets, we propose an efficient method, called the *CenterLeaping*. The optimization objective can be summarized as reducing the distance between the tracklet and the target object. As the bboxes are computed with discrete locations of heat points in the heatmap, we cannot directly optimize the loss of bboxes to make them close to each other. So the goal is achieved by reducing the distance between the centers of bboxes, as well as the differences of their sizes and offsets. Hence, the detection optimization function for the attack trajectory k can be expressed as follows:

$$\begin{aligned} \min \sum_{k \in \{i,j\}} d_{box}(K(m_{t-1}^{\tilde{k}}), box_t^k) \\ = \min \sum_{k \in \{i,j\}} \left(d(cet(K(m_{t-1}^{\tilde{k}})), cet(box_t^k)) + \right. \\ \left. d(size(K(m_{t-1}^{\tilde{k}})), size(box_t^k)) + \right. \\ \left. d(off(K(m_{t-1}^{\tilde{k}})), off(box_t^k)) \right), \end{aligned} \quad (5)$$

where m_{t-1}^k represents the motion state of the attack or screener tracklet, box_t^k represents the bbox of the attack or screener object, $d(\cdot)$ denotes the L_1 distance, $cet(\cdot)$, $size(\cdot)$ and $off(\cdot)$ compute the bbox's center, size and offset, respectively.

To make the object to be close to the center of the target tracklet, based on the focal loss of FairMOT, we design the *CenterLeaping* loss to let the center of the attack (screener) bbox move close to the screener (attack) trajectory (see Fig. 3c):

$$\mathcal{L}_{cl} = \sum_{k \in \{i,j\}} \left(\sum_{(x,y) \in \mathcal{B}_{c_{\tilde{k}}}} -(1 - M_{x,y})^\gamma \log(M_{x,y}) + \sum_{(x,y) \in \mathcal{B}_{c_k}} -(M_{x,y})^\gamma \log(1 - M_{x,y}) \right), \quad (6)$$

where $M_{x,y}$ represents the value of heatmap at location (x, y) , c_k represents the center of the attack or screener object, and $c_{\tilde{k}}$ represents the point in the direction from c_k to $cet(K(m_{t-1}^{\tilde{k}}))$. During the optimization iteration, point $c_{\tilde{k}}$

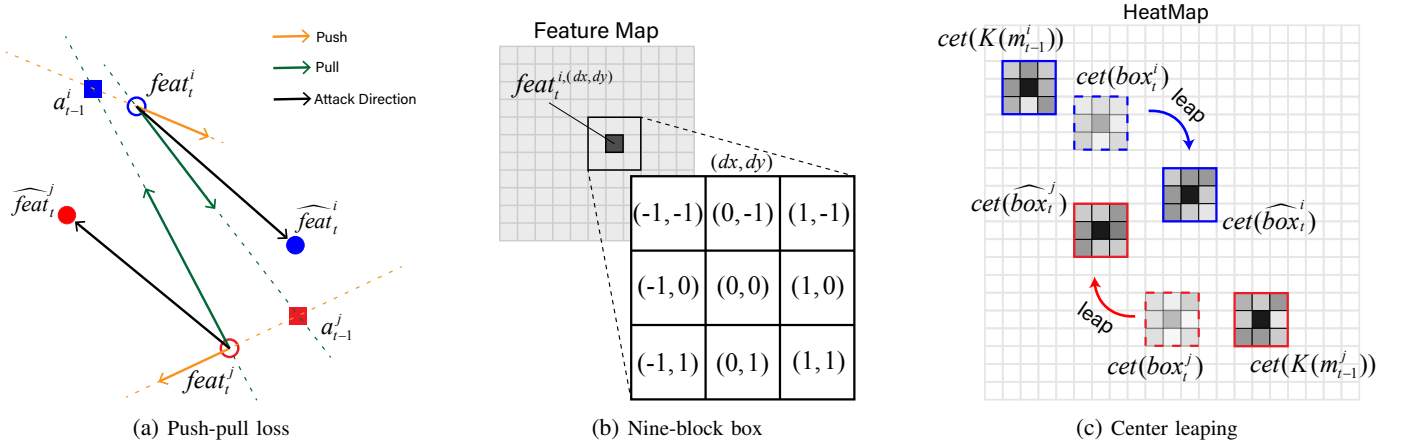


Fig. 3: The key components of TraSw. (a) The illustration of *PushPull* loss. The blue and red points represent different IDs to be attacked. The goal of the *PushPull* loss is to push the feature $feat_t^i$ of object i in frame t away from that of tracklet i , a_{t-1}^i , and to pull $feat_t^i$ to be close to another tracklet a_{t-1}^j ; and vice versa to $feat_t^j$. (b) The nine-block box (\mathcal{B}). The surrounding features are also used to calculate the loss. (c) The center leaping for the detection branch. The dotted boxes indicate the original heat points, which need to be cooled down; and the solid boxes in the t -th frame indicate the adversarial heat points, which need to be heated up. In this way, the $cet(box_t^i)$ and $cet(box_t^j)$ leaps to $cet(box_t^i)$ and $cet(box_t^j)$ along the direction of $cet(K(m_{t-1}^i))$ and $cet(K(m_{t-1}^j))$.

will leap to the next grid along the direction. As a result, the heatmap values around the original object centers get cooled down, while the points close to $cet(K(m_{t-1}^k))$ are warmed up.

We also restrain the sizes and offsets of the objects by a regression loss:

$$\begin{aligned} \mathcal{L}_{reg} &= \mathcal{L}_{size} + \mathcal{L}_{offset} \\ &= \sum_{k \in \{i,j\}} \mathcal{L}_1^{smooth}(size(K(m_{t-1}^k)), size(box_t^k)) + \\ &\quad \sum_{k \in \{i,j\}} \mathcal{L}_1^{smooth}(off(K(m_{t-1}^k)), off(box_t^k)), \end{aligned} \quad (7)$$

where \mathcal{L}_1^{smooth} denotes the smooth L_1 loss:

$$\mathcal{L}_1^{smooth}(a, b) = \begin{cases} 0.5 \cdot (a - b)^2 & \text{if } |a - b| < 1, \\ |a - b| - 0.5 & \text{else.} \end{cases} \quad (8)$$

C. Crafting the Adversarial Video

Summing up the above, we get the total loss for optimization:

$$\min_{\hat{V}} Loss = \min_{\hat{V}} \mathcal{L}_{pp} + \mathcal{L}_{cl} + \mathcal{L}_{reg}. \quad (9)$$

Then we can calculate the gradient of the total loss with an L_2 regularization:

$$\hat{I}_0 = I, \quad \hat{I}_{i+1} = Clip_{[0,1]} \left(\hat{I}_i - \frac{\nabla_{\hat{I}} Loss(\hat{I}_i; \theta)}{\|\nabla_{\hat{I}} Loss(\hat{I}_i; \theta)\|_2} \right), \quad (10)$$

where \hat{I}_i denotes the adversarial image at the i -th iteration.

The algorithm overview of crafting the adversarial videos is shown in Algorithm 1. First, we specify an attack trajectory ID_{att} in the original tracking video before the attack. For each coming frame, we initialize the tracklet pools, TrP_t and \widehat{TrP}_t , with the original frame, and initialize the adversarial frame \hat{I}_t as I_t . Second, we conduct a double check to determine whether to attack the current frame: 1) check whether the object of

trajectory ID_{att} has appeared for more than Thr_{frame} frames (10 in default) with $Exist(\cdot)$. This is because the overall attack will make no sense if the attack starts from the first appearance of the attack target; 2) check whether the tracking of the attack object is the same as the original video with $CheckFit(\cdot)$. If both conditions are satisfied, we then try to find an object that overlaps most with object ID_{att} as the screener object ID_{scr} by $FindMaxIoU(\cdot)$. Then we check whether the IoU between objects ID_{att} and ID_{scr} is greater than Thr_{IoU} . If true, the current frame will be attacked, and otherwise not.

For the attacking, we use the $NoiseGenerator(\cdot)$ to generate adversarial noise by optimizing Eq. (9) iteratively. In particular, for the *CenterLeaping* loss, when the number of iterations reaches 10, 20, 30, 35, 40, 45, 50 or 55, the heat point $c_{\nearrow k}$ will advance one grid towards c_k from its current position. $c_{\nearrow k}$ won't stop advancing until it overlaps with c_k . During each iteration of optimization and attack, a specific noise will be generated and added to the video frame by Eq. (10) until the tracker makes mistakes in the current iteration or the number of iterations reach Thr_{iter} (60 in default).

We add the noise to the current frame no matter whether the attack succeeds, and the experiments in Sec. V-C show that such operation contributes to an easier attack for the following frames. The tracklet pool \widehat{TrP}_t is then re-updated by the adversarial frame \hat{I}_t , and the threshold Thr_{IoU} is set to zero. In the end, the adversarial frame \hat{I}_t is added to the adversarial video \hat{V} .

V. EXPERIMENTS

In this section, we first introduce the experimental setup, then we present the results of TraSw and the baselines to demonstrate the effectiveness and efficiency of TraSw. Next, we analyze the importance of components in TraSw through the ablation study. In the end, we discuss the influence of Thr_{IoU} and present the distribution area of adversarial noise.

Algorithm 1: The TraSw Attack

Input: Video image sequence $V = \{I_1, \dots, I_N\}$; MOT $Tracker(\cdot)$; attack ID ID_{att} ; attack IoU threshold Thr_{IoU} ; start attack frame Thr_{frame} ; maximum iteration Thr_{iter}

Output: Sequence of adversarial video \hat{V} ; original tracklet pool TrP_N ; adversarial tracklet pool \widehat{TrP}_N

```

1 Init  $\hat{V} \leftarrow \{\}$ ;  $TrP_0 \leftarrow None$ ;  $\widehat{TrP}_0 \leftarrow None$ 
2 for  $t=1$  to  $N$  do
3    $TrP_t \leftarrow Tracker(I_t, TrP_{t-1})$ ;
4    $\widehat{TrP}_t \leftarrow Tracker(I_t, \widehat{TrP}_{t-1})$ ;
5    $\hat{I}_t \leftarrow I_t$ ; ▷ initialize the outputs
6   ▷ check if the attack tracklet has been existed for at least  $Thr_{frame}$  frames and the object is tracked as  $ID_{att}$ 
7   if  $Exist(ID_{att}, TrP_t) > Thr_{frame}$  and  $CheckFit(TrP_t|ID_{att}, \widehat{TrP}_t|ID_{att})$  then
8     ▷ find the screener object that overlaps most with the attack object
9      $ID_{scr} \leftarrow FindMaxIoU(TrP_t, ID_{att})$ ;
10    if  $IoU(TrP_t|ID_{att}, TrP_t|ID_{scr}) > Thr_{IoU}$  then
11      ▷ generate adversarial noise iteratively with Eq. (10)
12       $noise \leftarrow NoiseGenerator(ID_{att}, ID_{scr}, I_t, TrP_t, \widehat{TrP}_{t-1}, Tracker(\cdot), Thr_{iter})$ ;
13       $\hat{I}_t \leftarrow Clip_{[0,1]}(I_t + noise)$ ; ▷ clip the adversarial image to  $[0, 1]$ 
14       $\widehat{TrP}_t \leftarrow Tracker(\hat{I}_t, \widehat{TrP}_{t-1})$ ; ▷ update the adversarial tracklet
15       $Thr_{IoU} \leftarrow 0$ ; ▷ set  $Thr_{IoU}$  to 0 if start to attack
16    end
17  end
18   $\hat{V} \leftarrow \hat{V} \cup \hat{I}_t$ ; ▷ update the adversarial video
19 end

```

A. Experimental Setup

Target Models and Datasets. We choose two representative trackers as the target models: FairMOT [35] and ByteTrack [29]. FairMOT is also used for ablation studies. In particular, we only use *CenterLeaping* to attack ByteTrack, as there is no re-ID branch in ByteTrack. We validate TraSw on the test sets of three benchmarks: 2DMOT15 [36], MOT17 [37] and MOT20 [38].

Baselines. TraSw is compared with three classic baselines: 1) random noise perturbation (denoted as RanAt) whose L_2 distance per frame is limited to $[2, 8]$ randomly; 2) detection attack (denoted as DetAt) which aims to make the attack object invisible to the object detection module [15], [22], [23], [39] (commonly used in object detection and SOT attacks); 3) *tracker hijacking* attack (denoted as Hijack) [25].

Evaluation Metric. Similar to [25], an attack is regarded as successful when the detected objects of the attack trajectory are no longer associated with the original tracklet after the attack. As described in Sec. IV-C, our method attacks when an object overlaps with the attack object. So the attack success rate depends on two factors. Firstly, we need to obtain the number of trajectories satisfying the attack conditions: 1) the trajectory’s object should have appeared for at least Thr_{frame} (10 as the default value) frames; 2) there exists another object overlapping with the attack object, and the IoU should be greater than Thr_{IoU} (0.2 as the default value). Secondly, we need to obtain the number of successfully attacked trajectories for which the detected bboxes are no longer associated with the original tracklets after the attack. For comparison purposes, the attack conditions of the baselines are the same as TraSw. The

effectiveness and efficiency of our method are demonstrated through the attack success rate ($Succ.$ \uparrow), attacked frames ($\#Fm.$ \downarrow), and L_2 distance (L_2 \downarrow) per track ID of the successful attacks. To make the attack more efficient, the attacked frames are limited to at most 20.

B. Adversarial Attack Results

We report the results of TraSw and the baselines on the test datasets of 2DMOT15, MOT17, and MOT20. The results are as shown in Table I.

Column IDS_{att} is the number of the attackable trajectories on the given tracker and dataset. From the experimental results, we can observe that:

- Compared with the baselines, TraSw achieves the highest $Succ.$ on the three datasets with fewer frames $\#Fm.$ and smaller perturbations L_2 .
- Generally, in the crowded pedestrian tracking scenarios (MOT20), TraSw can achieve a higher success rate than that in the normal scenarios (2DMOT15 and MOT17) while DetAt and Hijack do not have significant improvement. In summary, the results indicate the effectiveness of TraSw in attacking the pedestrian multi-object trackers.
- Hijack seems not adaptable to pedestrian multi-object trackers, especially on the crowded pedestrian datasets (MOT20). TraSw, by contrast, has outstanding performance on all the three benchmarks.
- For ByteTrack, which has better tracking ability, TraSw seems more stable while the success rates of other baselines decrease significantly.

In addition, we also compare the attack results under the constraints of attacked frames and L_2 distance (see Fig. 4).

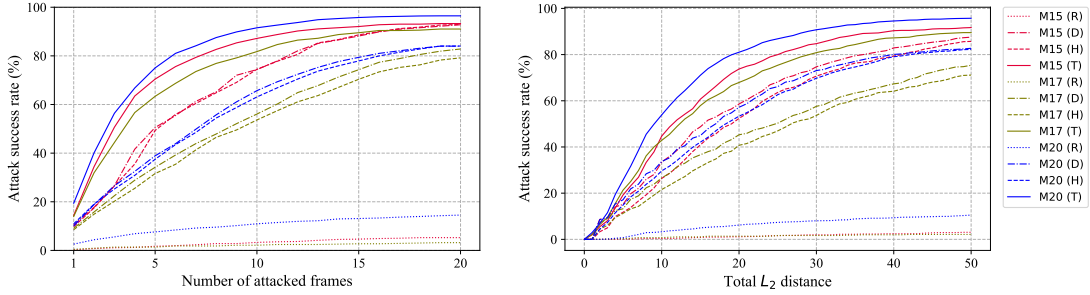


Fig. 4: The evaluation results of trackers attacked by RanAt (R), DetAt (D), Hijack (H) and TraSw (T) on 2DMOT15 (M15), MOT17 (M17) and MOT20 (M20), respectively.

TABLE I: Comparison of the attacks on the MOT-Challenge test datasets.

Dataset	Tracker	Method	$Succ. \uparrow$ (%)	$\#Fm. \downarrow$	$L_2 \downarrow$	$ID_{s_{att}}$
2DMOT15	FairMOT	RanAt	5.25	8.74	43.85	820
		DetAt	92.80	6.43	19.17	
		Hijack	92.92	6.57	21.74	
		TraSw	93.28	4.25	13.99	
	ByteTrack	RanAt	4.80	6.83	34.14	730
		DetAt	85.09	5.98	36.65	
		Hijack	81.89	6.85	38.57	
		TraSw	89.88	4.09	26.49	
MOT17	FairMOT	RanAt	3.19	7.57	37.50	658
		DetAt	82.83	7.84	23.07	
		Hijack	79.18	8.00	24.39	
		TraSw	91.03	4.74	14.40	
	ByteTrack	RanAt	4.26	7.73	40.14	705
		DetAt	70.35	6.04	27.81	
		Hijack	67.53	6.95	32.31	
		TraSw	91.06	4.17	24.02	
MOT20	FairMOT	RanAt	14.53	6.77	34.17	1892
		DetAt	83.99	6.81	16.31	
		Hijack	84.04	7.09	17.88	
		TraSw	96.46	3.94	11.67	
	ByteTrack	RanAt	4.27	7.46	37.07	1899
		DetAt	61.93	7.32	33.63	
		Hijack	58.66	8.18	30.25	
		TraSw	94.84	3.46	19.54	

Compared with the baselines, TraSw yields higher success rates at certain attacked frames and L_2 distance constraints on the three datasets.

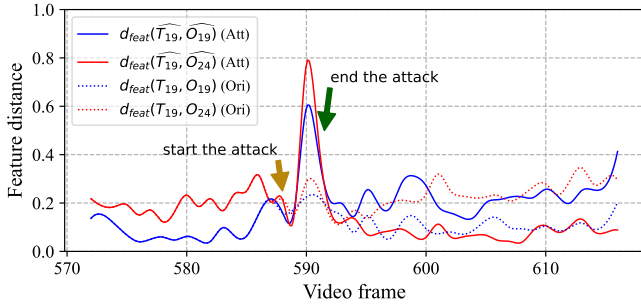
To better understand TraSw, we provide analysis on the attacking instance illustrated in Fig. 1 for the 19-th tracklet (24-th tracklet is the screener object). Specifically, we plot the feature distance and box distance trends in Fig. 5. The blue lines indicate the distance between tracklet 19 and object with the original ID of 19. The red lines indicate the distance between tracklet 19 and object with the original ID of 24. The solid lines and the dotted lines indicate the trend curve in the adversarial video and the original video. We can observe that the solid lines coincide with the dotted lines before the attack, yet after the attack, the red line and the blue line of the

adversarial video switch, and tracklet 19 is instead similar to object 24. The original intention of updating tracklets at each time step is to adapt to variations of the tracked objects, but the update mechanism of tracklets allows us to tamper with the tracklets so that the tracker does not realize of tracking a completely different object.

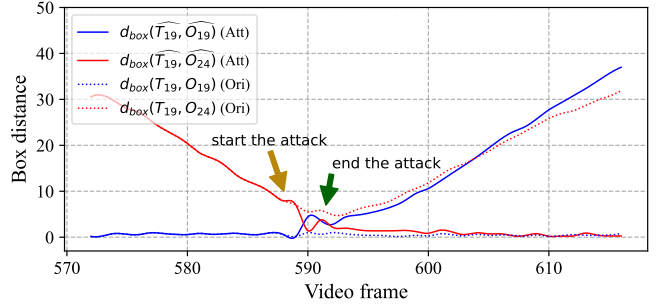
C. Ablation Study

Here we discuss the necessity of *PushPull*, *CenterLeaping*, and *Adding Failing Noise*. The comparisons are conducted on FairMOT to analyze the contribution of each component in TraSw. The results are shown in Table II.

From the results, we can observe that:



(a) Feature distances in the video



(b) Box distances in the video

Fig. 5: Distances of features and boxes in the original video and adversarial video. d_{feat} and d_{box} represent the cosine similarity of features and the Mahalanobis distance of boxes, as presented in Sec. III-A. \widehat{T}_{id} (\widehat{O}_{id}) and T_{id} (O_{id}) denote the adversarial and original tracklets (objects).

TABLE II: Attack success rates at certain attack frames. PP , CL and FN represent the *PullPush*, *CenterLeaping* and *Adding Failure Noise*, respectively. $n_{\#Fm.}$ presents attacking at most n frames.

Dataset	Attackers	Attack success rate \uparrow (%)				
		$1_{\#Fm.}$	$5_{\#Fm.}$	$10_{\#Fm.}$	$15_{\#Fm.}$	$20_{\#Fm.}$
2DMOT15	TraSw w/o PP	11.4	61.1	83.5	90.2	93.2
	TraSw w/o CL	11.2	67.1	87.6	91.6	92.8
	TraSw w/o FN	17.8	66.8	82.9	85.6	87.2
	TraSw	14.4	70.5	87.8	92.1	93.3
MOT17	TraSw w/o PP	9.7	51.1	75.0	85.9	90.0
	TraSw w/o CL	8.8	38.5	64.7	74.6	81.2
	TraSw w/o FN	15.5	62.3	79.3	85.9	89.1
	TraSw	14.0	63.4	81.8	89.5	91.0
MOT20	TraSw w/o PP	13.0	64.6	86.8	93.2	94.0
	TraSw w/o CL	11.2	50.8	74.5	82.2	84.8
	TraSw w/o FN	20.9	72.3	88.8	92.9	93.3
	TraSw	19.4	75.1	91.5	95.8	96.5

- The performance of TraSw without PP/CL is much worse than the overall TraSw when only a few frames are attacked (*i.e.*, $1_{\#Fm.}$ and $5_{\#Fm.}$), especially on MOT17 and MOT20. It shows that *PullPush* together with *CenterLeaping* can significantly reduce the attacked frames.
- The performance of TraSw without FN is greatly suppressed as the number of attacked frames increases. It shows that *Adding Failing Noise* can make the later frames easier to be attacked, especially on 2DMOT15. However, with only one frame being attacked, TraSw without FN seems better than the overall TraSw. The unsuccessfully attacked frame will be disturbed with the *failing noise* for the overall TraSw but not for the TraSw without FN . And a frame without noise will not be seen as an attacked frame. Therefore, the attack success rate of TraSw without FN seems slightly higher than the overall TraSw for only one attacked frame.
- On MOT17 and MOT20, the attack success rate of TraSw without CL drops more than that without PP , indicating that *CenterLeaping* can further improve the attack success rate in crowded scenarios. It seems that the bounding box

matching mechanism of the association algorithm, which is widely used in MOT, is more vulnerable.

In summary, the three components of TraSw significantly contribute to the great performance.

D. Parameter Study on IoU Threshold

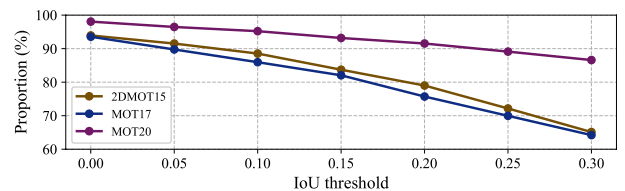


Fig. 6: Proportion of attackable objects.

One of the TraSw's attack conditions is that there is another object overlapping with the attack object, and the IoU is greater than the threshold Thr_{IoU} . It seems that the attack condition makes TraSw relatively limited (*i.e.*, a few objects satisfy the attack condition). However, according to our analysis in Fig. 6, in most scenarios, the attackable objects occupy 80% under the experimental Thr_{IoU} of 0.2; it is even

as high as 90% in the dense scenarios (MOT20). Hence, our approach can adapt to most pedestrian tracking scenarios.

E. Noise Pattern



Fig. 7: The distribution area of noise.

As shown in Fig. 7, five attack tracklets are randomly selected from five videos to show the distribution area of noise. The blue boxes and red boxes represent the attack and screener objects. The noise mainly focuses on the attack and screener objects, leaving other regions almost not perturbed. It demonstrates that TraSw can focus on key areas and attack the frames efficiently.

VI. DISCUSSION AND FUTURE WORK

In this section, we firstly discuss how to extend TraSw to other MOT trackers. Then according to the experimental results, we provide some possible defensive directions. Finally, we propose future work in terms of robustness.

A. Discussion on Attack Extension

In this work, we study the adversarial attack against MOT trackers and choose two representative types of trackers [29], [35] to analyze and attack. As for other similarly structured MOT trackers [1], [31], [33], [50]–[52] (*i.e.*, detection-based trackers or motion-and-appearance-based trackers), TraSw can transplant on them with almost nothing to change. But for some different-structured models [32], [53]–[55], TraSw should be changed to adapt to these models based on the optimization goal described in Sec. III-B, which aims to switch the appearance and distance similarity of the intersecting trajectories.

Take CenterTrack [32] for example. CenterTrack takes two adjacent frames and the heat map from the previous frame as input and outputs an extra displacement prediction map compared to CenterNet [48]. It is similar to the optical flow method that the displacement prediction map aims to predict the displacement of the center points of the detection frame in the front and back frames:

$$\mathcal{L}_{Dis} = \frac{1}{N} \sum_{i=1}^N \left| \hat{D}_{p_i^t} - (p_i^{t-1} - p_i^t) \right|, \quad (11)$$

where $\hat{D}_{p_i^t}$ denotes the value of the 2D displacement prediction map $\hat{D} \in \mathbb{R}^{\frac{W}{4} \times \frac{H}{4} \times 2}$ at location of the i -th detected object in the t -th frame p_i^t , p_i^{t-1} and p_i^t are the tracked ground-truth objects. In order to perturb such models and switch the

trajectories, TraSw needs to make some adjustments to adapt to CenterTrack:

$$\min_{\hat{D}} \left| \hat{D}_{p_i^t} - (p_j^{t-1} - p_i^t) \right| + \left| \hat{D}_{p_j^t} - (p_i^{t-1} - p_j^t) \right| \quad (12)$$

and

$$\max_{\hat{D}} \left| \hat{D}_{p_i^t} - (p_i^{t-1} - p_i^t) \right| + \left| \hat{D}_{p_j^t} - (p_j^{t-1} - p_j^t) \right|, \quad (13)$$

where i, j represent the attack and screener objects.

Theoretically, TraSw is not limited to the pedestrian Multi-Object Tracking systems. The scene of intersecting objects also appears in other Multi-Object Tracking tasks, such as autonomous driving [56]–[59], multi-target multi-camera tracking [60]–[63], *etc.* Therefore, our attack method TraSw can also be migrated to these tasks. Although these scenes may not have as many intersecting objects as pedestrian Multi-Object Tracking has, the robustness of models in the case of object intersection cannot be ignored. We will continue to explore our methods on other scenarios like vehicle tracking in our future work.

Considering that those MOT systems are not as popular and high-precision as FairMOT and ByteTrack, we did not apply TraSw to them yet. In this work, we argue that ”when to attack” is more important than ”how to attack”, and propose an attack method called TraSw. The existing white-box attack methods [7], [64], [65] and even black-box attack methods [66]–[68] on classification can be implemented in our method.

The ID switch is important in MOT tasks, and our method gains great achievement on online trackers. However, offline trackers can recover incorrectly matched tracklets, and how to attack the offline trackers effectively would be another possible line of future work.

B. Discussion on Possible Defense

TraSw can effectively make two intersecting trajectories switch with imperceptible perturbations. How can we defend such attack? There are usually two ways to defend adversarial attacks: 1) identify the adversarial examples and deal with them (denoise or discard) [69]–[71]; 2) improve the robustness of models [7], [72], [73]. The first usually reduces the model accuracy and takes extra time. Based on our experimental results, we mainly discuss how to improve the robustness of trackers.

Through the above experiments, something interesting enlightens us in the defensive direction. In real-world scenarios, obviously, trackers need to distinguish different pedestrians with appearance embeddings, especially when pedestrians intersect. However, the process of attack in Fig. 5a and the ablation study in Sec. V-C show that the re-ID features of FairMOT are not discriminative enough. Take the instance in Fig. 1 for example. The cosine similarity of the deep appearance features even switches without attack (see the dotted line in Fig. 5a). Besides, the attack success rates of TraSw without *PullPush* reach the same level as the overall TraSw as compared with TraSw without *CenterLeaping* (see Sec. V-C). It shows that only attacking the detection branch

can achieve a high success rate, and the re-ID branch does not work very well when the target boxes are close to each other. Therefore, improving the robustness of re-ID branch can be used as a way of defense.

The association algorithm widely used by the state-of-the-art trackers [29], [35], [50], [53], [74] also has some defects. The algorithm aims to get the global optimal with the Hungarian algorithm in each matching phase. However, for hard samples at the decision boundary, such as the close pedestrians, the algorithm is prone to errors with adversarial examples. The tracker will continue tracking the wrong trajectories without realizing the error. Hence, robustness of the association algorithm should be improved to defend against such imperceptible perturbations.

C. Future Work

The study of adversarial examples is of great importance to the model robustness. In future work, we will follow up this direction and continue to explore the following problems.

MOT often needs to handle the complex data association problem. Instead of attacking the model with a simple negative optimization method, we explore the vulnerability of MOT models from different perspectives. In this work, we propose a new attack method called TraSw under ideal scenarios, and more researches in real-world scenarios worth further exploration.

In addition to the pedestrian multi-object tracking system, we will try to apply TraSw to more Multi-Object Tracking scenarios as discussed in Sec. VI-A. We believe that the robustness of all Multi-Object Tracking tasks, which exist intersecting objects, needs to be investigated and improved.

We hope that the proposed attack method could inspire more works in designing robust MOT trackers. We will also continue to design adversarial defense methods to improve the robustness of existing MOT models. As discussed in Sec. VI-B, we will also study the robustness from the defensive point of view and design an MOT system that includes redesigned feature extraction modules and post-processing algorithms.

VII. CONCLUSION

To our knowledge, this is the first work to study the adversarial attack against pedestrian MOT trackers. The proposed adversarial attack method, TraSw, which consists of the *PushPull* and *CenterLeaping* techniques, can efficiently deceive the advanced MOT trackers at a high success rate. Exploiting the update mechanism of tracklets to attack the MOT trackers, TraSw also demonstrates the weakness of the re-ID branch and the association algorithm in MOT systems. Empirical experiments on standard benchmarks show that our method outperforms the existing attack methods on object detection. Considering that this is the first adversarial study on pedestrian MOT, we also provide the comparison with *tracker hijacker*, which is focused on vehicle MOT, for reference. Our work shows the effectiveness and great potential of the proposed method for MOT trackers.

ACKNOWLEDGMENT

This work is supported by National Natural Science Foundation (U22B2017, 62076105).

REFERENCES

- [1] N. Wojke, A. Bewley, and D. Paulus, "Simple online and realtime tracking with a deep association metric," in *2017 IEEE International Conference on Image Processing (ICIP)*, 2017, pp. 3645–3649.
- [2] L. Chen, H. Ai, Z. Zhuang, and C. Shang, "Real-time multiple people tracking with deeply learned candidate selection and person re-identification," in *2018 IEEE International Conference on Multimedia and Expo (ICME)*, 2018, pp. 1–6.
- [3] X. Li, W. Hu, C. Shen, Z. Zhang, A. Dick, and A. V. D. Hengel, "A survey of appearance models in visual object tracking," *ACM Transactions on Intelligent Systems and Technology (TIST)*, vol. 4, no. 4, pp. 1–48, 2013.
- [4] R. Xu, S. Y. Nikouei, Y. Chen, A. Polunchenko, S. Song, C. Deng, and T. R. Faughnan, "Real-time human objects tracking for smart surveillance at the edge," in *2018 IEEE International Conference on Communications (ICC)*, 2018, pp. 1–6.
- [5] J. Candamo, M. Shreve, D. B. Goldgof, D. B. Sapper, and R. Kasturi, "Understanding transit scenes: A survey on human behavior-recognition algorithms," *IEEE Transactions on Intelligent Transportation Systems*, vol. 11, no. 1, pp. 206–224, 2009.
- [6] C. Szegedy, W. Zaremba, I. Sutskever, J. Bruna, D. Erhan, I. J. Goodfellow, and R. Fergus, "Intriguing properties of neural networks," in *International Conference on Learning Representations (ICLR)*, 2014.
- [7] I. J. Goodfellow, J. Shlens, and C. Szegedy, "Explaining and harnessing adversarial examples," *arXiv preprint arXiv:1412.6572*, 2014.
- [8] A. Kurakin, I. J. Goodfellow, and S. Bengio, "Adversarial examples in the physical world," in *Artificial Intelligence Safety and Security*. Chapman and Hall/CRC, 2018, pp. 99–112.
- [9] K. Eykholt, I. Evtimov, E. Fernandes, B. Li, A. Rahmati, C. Xiao, A. Prakash, T. Kohno, and D. Song, "Robust physical-world attacks on deep learning visual classification," in *Proceedings of the IEEE/CVF Conference on Computer Vision and Pattern Recognition (CVPR)*, 2018, pp. 1625–1634.
- [10] Y. Zhao, H. Zhu, R. Liang, Q. Shen, S. Zhang, and K. Chen, "Seeing isn't believing: Towards more robust adversarial attack against real world object detectors," in *Proceedings of the 2019 ACM SIGSAC Conference on Computer and Communications Security*, 2019, pp. 1989–2004.
- [11] A. Nguyen, J. Yosinski, and J. Clune, "Deep neural networks are easily fooled: High confidence predictions for unrecognizable images," in *Proceedings of the IEEE/CVF Conference on Computer Vision and Pattern Recognition (CVPR)*, 2015, pp. 427–436.
- [12] C. Szegedy, W. Zaremba, I. Sutskever, J. Bruna, D. Erhan, I. J. Goodfellow, and R. Fergus, "Intriguing properties of neural networks," in *International Conference on Learning Representations (ICLR)*, 2014.
- [13] S.-M. Moosavi-Dezfooli, A. Fawzi, O. Fawzi, and P. Frossard, "Universal adversarial perturbations," in *Proceedings of the IEEE/CVF Conference on Computer Vision and Pattern Recognition (CVPR)*, 2017, pp. 1765–1773.
- [14] J. Lin, C. Song, K. He, L. Wang, and J. E. Hopcroft, "Nesterov accelerated gradient and scale invariance for adversarial attacks," in *International Conference on Learning Representations (ICLR)*, 2020.
- [15] J. Lu, H. Sibai, and E. Fabry, "Adversarial examples that fool detectors," *arXiv preprint arXiv:1712.02494*, 2017.
- [16] J. Bao, "Sparse adversarial attack to object detection," *arXiv preprint arXiv:2012.13692*, 2020.
- [17] S.-T. Chen, C. Cornelius, J. Martin, and D. H. P. Chau, "Shapeshifter: Robust physical adversarial attack on faster r-cnn object detector," in *Machine Learning and Knowledge Discovery in Databases*, 2019, pp. 52–68.
- [18] Y.-C.-T. Hu, B.-H. Kung, D. S. Tan, J.-C. Chen, K.-L. Hua, and W.-H. Cheng, "Naturalistic physical adversarial patch for object detectors," in *Proceedings of the IEEE/CVF International Conference on Computer Vision (ICCV)*, 2021, pp. 7848–7857.
- [19] C. Xie, J. Wang, Z. Zhang, Y. Zhou, L. Xie, and A. Yuille, "Adversarial examples for semantic segmentation and object detection," in *Proceedings of the IEEE/CVF International Conference on Computer Vision (ICCV)*, 2017, pp. 1369–1378.
- [20] J. Hendrik Metzen, M. Chaithanya Kumar, T. Brox, and V. Fischer, "Universal adversarial perturbations against semantic image segmentation," in *Proceedings of the IEEE/CVF Conference on Computer Vision and Pattern Recognition (CVPR)*, 2017, pp. 2755–2764.

- [21] V. Fischer, M. C. Kumar, J. H. Metzen, and T. Brox, “Adversarial examples for semantic image segmentation,” in *5th International Conference on Learning Representations, ICLR 2017, Workshop Track Proceedings*, 2017.
- [22] X. Chen, X. Yan, F. Zheng, Y. Jiang, S.-T. Xia, Y. Zhao, and R. Ji, “One-shot adversarial attacks on visual tracking with dual attention,” in *Proceedings of the IEEE/CVF Conference on Computer Vision and Pattern Recognition (CVPR)*, 2020, pp. 10 176–10 185.
- [23] B. Yan, D. Wang, H. Lu, and X. Yang, “Cooling-shrinking attack: Blinding the tracker with imperceptible noises,” in *Proceedings of the IEEE/CVF Conference on Computer Vision and Pattern Recognition (CVPR)*, 2020, pp. 990–999.
- [24] S. Jia, Y. Song, C. Ma, and X. Yang, “IoU attack: Towards temporally coherent black-box adversarial attack for visual object tracking,” in *Proceedings of the IEEE/CVF Conference on Computer Vision and Pattern Recognition (CVPR)*, 2021, pp. 6709–6718.
- [25] Y. Jia, Y. Lu, J. Shen, Q. A. Chen, Z. Zhong, and T. Wei, “Fooling detection alone is not enough: First adversarial attack against multiple object tracking,” in *International Conference on Learning Representations (ICLR)*, 2020.
- [26] F. Yu, W. Li, Q. Li, Y. Liu, X. Shi, and J. Yan, “Poi: Multiple object tracking with high performance detection and appearance feature,” in *Proceedings of the European Conference on Computer Vision (ECCV)*, 2016, pp. 36–42.
- [27] W. Li, J. Mu, and G. Liu, “Multiple object tracking with motion and appearance cues,” in *Proceedings of the IEEE/CVF International Conference on Computer Vision Workshops (ICCVW)*, 2019, pp. 0–0.
- [28] L. Sommer, W. Krüger, and M. Teutsch, “Appearance and motion based persistent multiple object tracking in wide area motion imagery,” in *Proceedings of the IEEE/CVF International Conference on Computer Vision (ICCV)*, 2021, pp. 3878–3888.
- [29] Y. Zhang, P. Sun, Y. Jiang, D. Yu, Z. Yuan, P. Luo, W. Liu, and X. Wang, “ByteTrack: Multi-object tracking by associating every detection box,” *arXiv preprint arXiv:2110.06864*, 2021.
- [30] W. Luo, J. Xing, A. Milan, X. Zhang, W. Liu, and T.-K. Kim, “Multiple object tracking: A literature review,” *Artificial Intelligence*, p. 103448, 2020.
- [31] Z. Wang, L. Zheng, Y. Liu, Y. Li, and S. Wang, “Towards real-time multi-object tracking,” in *Proceedings of the European Conference on Computer Vision (ECCV)*, 2020, pp. 107–122.
- [32] X. Zhou, V. Koltun, and P. Krähenbühl, “Tracking objects as points,” in *Proceedings of the European Conference on Computer Vision (ECCV)*, 2020, pp. 474–490.
- [33] A. Bewley, Z. Ge, L. Ott, F. Ramos, and B. Upcroft, “Simple online and realtime tracking,” in *2016 IEEE International Conference on Image Processing (ICIP)*, 2016, pp. 3464–3468.
- [34] J. H. Yoon, C.-R. Lee, M.-H. Yang, and K.-J. Yoon, “Online multi-object tracking via structural constraint event aggregation,” in *Proceedings of the IEEE/CVF Conference on Computer Vision and Pattern Recognition (CVPR)*, 2016, pp. 1392–1400.
- [35] Y. Zhang, C. Wang, X. Wang, W. Zeng, and W. Liu, “Fairmot: On the fairness of detection and re-identification in multiple object tracking,” *International Journal of Computer Vision (IJCV)*, pp. 1–19, 2021.
- [36] L. Leal-Taixé, A. Milan, I. Reid, S. Roth, and K. Schindler, “MOTChallenge 2015: Towards a benchmark for multi-target tracking,” *arXiv preprint arXiv:1504.01942*, 2015.
- [37] A. Milan, L. Leal-Taixé, I. Reid, S. Roth, and K. Schindler, “MOT16: A benchmark for multi-object tracking,” *arXiv preprint arXiv:1603.00831*, 2016.
- [38] P. Dendorfer, H. Rezatofighi, A. Milan, J. Shi, D. Cremers, I. Reid, S. Roth, K. Schindler, and L. Leal-Taixé, “MOT20: A benchmark for multi object tracking in crowded scenes,” *arXiv preprint arXiv:2003.09003*, 2020.
- [39] Q. Guo, Z. Li, W. Xue, and W. Feng, “Spark: Spatial-aware online incremental attack against visual tracking,” in *Proceedings of the European Conference on Computer Vision (ECCV)*, 2020.
- [40] P. Sun, J. Cao, Y. Jiang, Z. Yuan, S. Bai, K. Kitani, and P. Luo, “Dancetrack: Multi-object tracking in uniform appearance and diverse motion,” in *Proceedings of the IEEE/CVF Conference on Computer Vision and Pattern Recognition*, 2022, pp. 20993–21 002.
- [41] S. Giancola, M. Amine, T. Dghaily, and B. Ghanem, “Soccernet: A scalable dataset for action spotting in soccer videos,” in *Proceedings of the IEEE Conference on Computer Vision and Pattern Recognition Workshops*, 2018, pp. 1711–1721.
- [42] J. Cai, M. Xu, W. Li, Y. Xiong, W. Xia, Z. Tu, and S. Soatto, “Memot: multi-object tracking with memory,” in *Proceedings of the IEEE/CVF Conference on Computer Vision and Pattern Recognition*, 2022, pp. 8090–8100.
- [43] S. Li, Y. Kong, and H. Rezatofighi, “Learning of global objective for network flow in multi-object tracking,” in *Proceedings of the IEEE/CVF Conference on Computer Vision and Pattern Recognition*, 2022, pp. 8855–8865.
- [44] G. Wang, R. Gu, Z. Liu, W. Hu, M. Song, and J.-N. Hwang, “Track without appearance: Learn box and tracklet embedding with local and global motion patterns for vehicle tracking,” in *Proceedings of the IEEE/CVF International Conference on Computer Vision (ICCV)*, 2021, pp. 9876–9886.
- [45] B. Li, J. Yan, W. Wu, Z. Zhu, and X. Hu, “High performance visual tracking with siamese region proposal network,” in *Proceedings of the IEEE/CVF Conference on Computer Vision and Pattern Recognition (CVPR)*, 2018, pp. 8971–8980.
- [46] B. Li, W. Wu, Q. Wang, F. Zhang, J. Xing, and J. Yan, “Siamrpn++: Evolution of siamese visual tracking with very deep networks,” in *Proceedings of the IEEE/CVF Conference on Computer Vision and Pattern Recognition (CVPR)*, 2019, pp. 4282–4291.
- [47] Z. Zhang and H. Peng, “Deeper and wider siamese networks for real-time visual tracking,” in *Proceedings of the IEEE/CVF Conference on Computer Vision and Pattern Recognition (CVPR)*, 2019, pp. 4591–4600.
- [48] K. Duan, S. Bai, L. Xie, H. Qi, Q. Huang, and Q. Tian, “Centernet: Keypoint triplets for object detection,” in *Proceedings of the IEEE/CVF International Conference on Computer Vision (ICCV)*, 2019, pp. 6569–6578.
- [49] F. Schroff, D. Kalenichenko, and J. Philbin, “FaceNet: A unified embedding for face recognition and clustering,” in *Proceedings of the IEEE/CVF Conference on Computer Vision and Pattern Recognition (CVPR)*, 2015, pp. 815–823.
- [50] Y. Du, Y. Song, B. Yang, and Y. Zhao, “Strongsort: Make deepsort great again,” *arXiv preprint arXiv:2202.13514*, 2022.
- [51] J. Cao, X. Weng, R. Khirodkar, J. Pang, and K. Kitani, “Observation-centric sort: Rethinking sort for robust multi-object tracking,” *arXiv preprint arXiv:2203.14360*, 2022.
- [52] C. Liang, Z. Zhang, X. Zhou, B. Li, S. Zhu, and W. Hu, “Rethinking the competition between detection and reid in multiobject tracking,” *IEEE Transactions on Image Processing*, vol. 31, pp. 3182–3196, 2022.
- [53] P. Chu, J. Wang, Q. You, H. Ling, and Z. Liu, “Transmot: Spatial-temporal graph transformer for multiple object tracking,” *arXiv preprint arXiv:2104.00194*, 2021.
- [54] J. Peng, C. Wang, F. Wan, Y. Wu, Y. Wang, Y. Tai, C. Wang, J. Li, F. Huang, and Y. Fu, “Chained-tracker: Chaining paired attentive regression results for end-to-end joint multiple-object detection and tracking,” in *Proceedings of the European Conference on Computer Vision (ECCV)*, 2020.
- [55] B. Shuai, A. Berneshawi, X. Li, D. Modolo, and J. Tighe, “Siammot: Siamese multi-object tracking,” in *Proceedings of the IEEE/CVF Conference on Computer Vision and Pattern Recognition (CVPR)*, June 2021, pp. 12 372–12 382.
- [56] S. Kato, S. Tokunaga, Y. Maruyama, S. Maeda, M. Hirabayashi, Y. Kit-sukawa, A. Monrroy, T. Ando, Y. Fujii, and T. Azumi, “Autoware on board: Enabling autonomous vehicles with embedded systems,” in *2018 ACM/IEEE 9th International Conference on Cyber-Physical Systems (ICPPS)*, 2018, pp. 287–296.
- [57] S. Kato, E. Takeuchi, Y. Ishiguro, Y. Ninomiya, K. Takeda, and T. Hamada, “An open approach to autonomous vehicles,” *IEEE Micro*, vol. 35, no. 6, pp. 60–68, 2015.
- [58] D. Zhao, H. Fu, L. Xiao, T. Wu, and B. Dai, “Multi-object tracking with correlation filter for autonomous vehicle,” *Sensors*, vol. 18, no. 7, p. 2004, 2018.
- [59] A. Ess, K. Schindler, B. Leibe, and L. Van Gool, “Object detection and tracking for autonomous navigation in dynamic environments,” *The International Journal of Robotics Research*, vol. 29, no. 14, pp. 1707–1725, 2010.
- [60] E. Ristani, F. Solera, R. Zou, R. Cucchiara, and C. Tomasi, “Performance measures and a data set for multi-target, multi-camera tracking,” in *Proceedings of the European Conference on Computer Vision (ECCV)*. Springer, 2016, pp. 17–35.
- [61] E. Ristani and C. Tomasi, “Features for multi-target multi-camera tracking and re-identification,” in *Proceedings of the IEEE/CVF Conference on Computer Vision and Pattern Recognition (CVPR)*, 2018, pp. 6036–6046.
- [62] Z. Zhang, J. Wu, X. Zhang, and C. Zhang, “Multi-target, multi-camera tracking by hierarchical clustering: Recent progress on dukemtmc project,” *arXiv preprint arXiv:1712.09531*, 2017.

- [63] A. Specker, D. Stadler, L. Florin, and J. Beyerer, “An occlusion-aware multi-target multi-camera tracking system,” in *Proceedings of the IEEE/CVF Conference on Computer Vision and Pattern Recognition (CVPR)*, 2021, pp. 4173–4182.
- [64] N. Carlini and D. A. Wagner, “Towards evaluating the robustness of neural networks,” *arXiv preprint arXiv:1608.04644*, 2016.
- [65] T. B. Brown, D. Mané, A. Roy, M. Abadi, and J. Gilmer, “Adversarial patch,” *arXiv preprint arXiv:1712.09665*, 2017.
- [66] N. Papernot, P. McDaniel, I. Goodfellow, S. Jha, Z. B. Celik, and A. Swami, “Practical black-box attacks against machine learning,” in *Proceedings of the 2017 ACM on Asia conference on computer and communications security*, 2017.
- [67] J. Yang, Y. Jiang, X. Huang, B. Ni, and C. Zhao, “Learning black-box attackers with transferable priors and query feedback,” *Advances in Neural Information Processing Systems*, 2020.
- [68] C. Guo, J. Gardner, Y. You, A. G. Wilson, and K. Weinberger, “Simple black-box adversarial attacks,” in *International Conference on Machine Learning (ICML)*. PMLR, 2019, pp. 2484–2493.
- [69] F. Liao, M. Liang, Y. Dong, T. Pang, X. Hu, and J. Zhu, “Defense against adversarial attacks using high-level representation guided denoiser,” in *Proceedings of the IEEE Conference on Computer Vision and Pattern Recognition*, 2018, pp. 1778–1787.
- [70] T. Pang, C. Du, and J. Zhu, “Max-mahalanobis linear discriminant analysis networks,” in *International Conference on Machine Learning (ICML)*. PMLR, 2018, pp. 4016–4025.
- [71] A. Nayebi and S. Ganguli, “Biologically inspired protection of deep networks from adversarial attacks,” *arXiv preprint arXiv:1703.09202*, 2017.
- [72] S. Sankaranarayanan, A. Jain, R. Chellappa, and S. N. Lim, “Regularizing deep networks using efficient layerwise adversarial training,” in *Proceedings of the AAAI Conference on Artificial Intelligence*, 2018.
- [73] A. Madry, A. Makelov, L. Schmidt, D. Tsipras, and A. Vladu, “Towards deep learning models resistant to adversarial attacks,” in *International Conference on Learning Representations (ICLR)*, 2018.
- [74] Q. Wang, Y. Zheng, P. Pan, and Y. Xu, “Multiple object tracking with correlation learning,” in *Proceedings of the IEEE/CVF Conference on Computer Vision and Pattern Recognition (CVPR)*, 2021.